PHILOSOPHICAL TRANSACTIONS OF THE ROYAL SOCIETY A MATHEMATICAL, PHYSICAL & ENGINEERING SCIENCES

Photodisplacement Techniques for Defect Detection [and Discussion]

Y. Martin, E. A. Ash, G. Busse and R. S. Gilmore

Phil. Trans. R. Soc. Lond. A 1986 **320**, 257-269
doi: 10.1098/rsta.1986.0115

Phil. Trans R. Soc. Lond. A **320**, 257–269 (1986)
Printed in Great Britain

Photodisplacement techniques for defect detection

By Y. Martin† and E. A. Ash, F.R.S.‡
Department of Electronic and Electrical Engineering, University College London, Torrington Place, London WC1E 7JE, U.K.

The absorption of a focused, modulated laser beam generates a thermal wave in a solid, the propagation of which is sensitive to the presence of surface or subsurface discontinuities. In the photodisplacement technique, one measures the periodic displacement of the object surface due to thermal expansion, with an interferometrical laser probe. Some instability problems of the probe are analysed and a modified version of it is described. A spatial resolution approaching that of conventional optical microscopy can be attained. Two basic effects play a role in the photodisplacement detection of defects: thermal-wave interaction and elastic deformation. As a consequence, the technique is particularly appropriate for the detection of 'physical' defects such as cracks, subsurface voids, and structural damage in a lattic such as caused by ion implantation. Images of such defects are presented. A novel photodisplacement configuration, where thermal-wave generation and detection are effected with a single laser, is described.

1. Introduction

'Photodisplacement' is a novel imaging technique based on the use of thermal waves in solids; the waves are generated by a modulated laser beam and detected by a second laser beam. The existence of thermal waves has been appreciated for over a century; these waves are highly attenuated, the 1/e range (proportional to $f^{-\frac{1}{2}}$), being typically of the order of a few micrometres at frequencies, f, between 10 kHz and 1 MHz.

The thermal effects can be detected at relatively long range by the fact that they are a source of acoustic waves. This leads to the concept of photoacoustic spectroscopy and imaging. We have evolved an alternative technique, photodisplacement, based on the detection of the thermal wave through the displacement that it engenders at the surface. The means for doing so that we have adopted, is to use a laser interferometer based on a second, low-power laser, having a different wavelength from that of the primary heating laser (figure 1).

We shall first describe the laser probe and its performance, along with some considerations of stability that have lead us to investigate a new optical configuration. We shall then in §3 examine some applications of the technique and identify some specific properties of materials that can be detected; preliminary results will be presented. We shall also introduce an alternative photodisplacement technique, where generation and detection of thermal waves are effected with a single laser, in §4.

† Present address: 22 Harrison Street, Clinton, New Jersey 08809, U.S.A.
‡ Present address: Imperial College, Prince Consort Road, London SW7 2AZ, U.K.

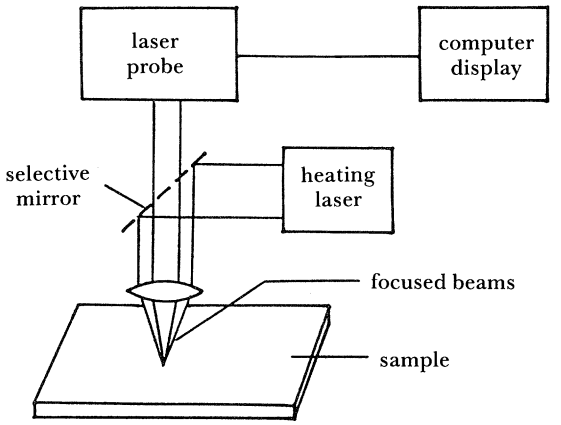

FIGURE 1. Photodisplacement diagram.

2. THE LASER PROBE: PERFORMANCE AND STABILITY

The laser probe is a highly sensitive instrument that measures surface displacements, such as can be obtained by surface acoustic waves (SAW) or by thermal expansion. It was first implemented by Whitman & Korpel (1969). It is now able to detect displacements at frequencies up to 500 MHz with a displacement sensitivity reaching 10^{-4} Å† (De la Rue *et al.* 1972). The probe acts as a heterodyne Michelson interferometer, in which one of the mirrors is the moving surface of the object to be examined. It measures periodic displacements of the surface in a prescribed band and is insensitive to frequencies which fall outside this band. By using a focused beam, the probe is made the basis of a microscope, capable of producing a diffraction limited digitized record of the complex distribution of a surface-displacement field.

Other schemes of Michelson interferometers have been used to measure vibrational amplitudes. Many require some sophisticated form of active stabilization (Olsson *et al.* 1980; Kwaaitaal *et al.* 1980), that are avoided by the heterodyne technique. Other probes, based on optical fibres, have also recently been developed, with similar sensitivity (Jungerman *et al.* 1982; Bowers *et al.* 1983); they are, however, more dependent to the surface reflectivity.

Figure 2 shows the diagram of the basic laser probe. It consists essentially of a Michelson interferometer based on a He–Ne laser. A Bragg cell replaces the usual beam splitter, and is driven so as to ensure that the intensity of the zero and the first order are approximately equal. The moving surface of the object reflects and phase modulates one of the beams. The mixing with the other beam occurs on the surface of a high frequency photodiode. The Bragg cell upconverts the optical frequency in the reference arm and down converts it in the signal arm by the Bragg-cell frequency. This introduces a carrier frequency at the photodiode, which is phase modulated by the surface displacement.

By using the complex description of light propagation, the optical field on the photodiode can be expressed as $(R+S)$, where R and S, shown in figure 2, are the reference and signal optical beams, that have been reflected respectively from the reference mirror and from the object. They are written as

$$R = r \exp\left(\mathrm{j}(\omega_0+\omega_B)\, t+\mathrm{j}\phi_R\right),$$

$$S = s \exp\left(\mathrm{j}(\omega_0-\omega_B)\, t+\mathrm{j}2kd \cos\left(\omega_m t+\phi_m\right)+\mathrm{j}\phi_S\right.$$

† $1\ \text{Å} = 10^{-1}\ \text{nm} = 10^{-10}\ \text{m}$.

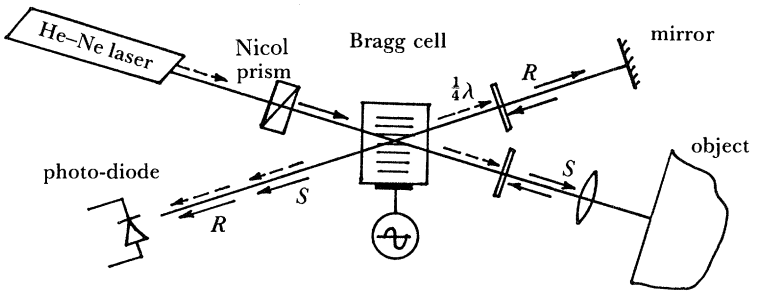

FIGURE 2. Optical configuration of the laser probe.

where r and s are constants; ω_0 is the optical frequency of the HeNe laser; ω_b is the Bragg cell frequency; ω_m is the surface displacement frequency of the object; k is the optical propagation constant; $k = \omega_0/c = 2\pi/\lambda$; d and ϕ_m are the amplitude and phase of the surface displacement; ϕ_R and ϕ_S are phase constants due to the optical path lengths in the reference and signal beams.

The optical power on the photodiode becomes

$$P = (R+S)\,(R+S)^*.$$

We obtain a value of P by expanding this expression in the first order for $kd \ll 1$ (in our case, $d < 10$ Å so that $kd < 10^{-2}$),

$$P = r^2 + s^2 + 2rs\cos(2\omega_B t + \phi_R - \phi_S) + kd\sin((2\omega_B + \omega_m)\,t + \phi_m + \phi_R - \phi_S) + kd\sin((2\omega_B - \omega_m)\,t - \phi_m + \phi_R - \phi_S).$$

The high-frequency components of P represent a phase modulated signal. They can be described as a carrier frequency at $2\omega_b$ plus two side bands separated by ω_m. These side bands contain the information on the surface displacement, the amplitude d and the phase ϕ_m. This optical section of the laser probe acts as a first heterodyne system. The signal on the photodiode is independent of the optical frequency ω_0. Therefore, any laser-frequency instability will not affect the laser probe signal. In addition, the electronic phase detection scheme operates by mixing the carrier and one of the sideband. This suppresses the dependency of the signal on the optical path length in ϕ_R and ϕ_S; thus, the surface displacement is free from any optical path length variations that fall outside of the detection bandwidth.

Two additional optical elements are shown in figure 2: a Nicol prism and a $\frac{1}{4}\lambda$ plate, that act as an isolator. The laser beam is linearly polarized; after passing twice through the $\frac{1}{4}\lambda$ plate, the direction of linear polarization has rotated by 90°. The Nicol prism then prevents its re-entry into the laser cavity, which otherwise would affect the laser output power. All the optical elements are mounted on a rigid metal bench. An air suspension isolates the bench from microphonic vibrations.

2.1. *The stability problem*

We have become aware of a major instability problem of the probe, which manifests itself by a slow temporal variation of the output signal that drastically reduces the dynamic range. The small amplitude of this variation, about 10% of the output signal, and its large time constant, typically around 1 s, made it difficult to trace its origin. The instability is different from white noise that could be due to shot or thermal effects; such a noise would be affected by the final bandwidth. However, the same level of instability is observed when the final bandwidth is varied from 1 kHz to 1 kHz. Simple effects, such as fluctuations of the laser power, or slow misalignments of the laser probe due to variations of temperature could also not explain

the instability; their main result is to introduce some amplitude variations at the photodiode, which are readily overcome by the use of a gain-controlled amplifier before the detection.

Three sources of instabilities having their origin in more complex light interactions, have been identified.

(i) *Back-reflection on the laser*

Under optimum alignment, the isolator (Nicol prism plus $\frac{1}{4}\lambda$ plates) has a maximum isolation of 23 dB, or a ratio 200 for the power. This means a ratio of only 14 for the amplitude of the electromagnetic field, which is what matters in the interference effect. Therefore, some light reflected from the sample or the reference mirror returns to the laser (dashed arrows on figure 1), despite the presence of the optical isolator. In particular, part of the beam coming from the reference mirror, is then reflected back by the front mirror of the laser. This spurious beam implies two other interfering beams on the detector. The resulting additional signal depends on the optical path lengths. Any path length variation due to temperature effect or slow movements of the air suspension will yield some instability. Up to 40 % of signal variation can at times be found from this effect alone.

(ii) *Spurious effect in the Bragg cell*

The Bragg cell provides a first-order beam with the optical frequency shifted by the frequency of the driving current, f_b. Other orders are generated, which are shifted by positive or negative multiples of f_b; they do not interfere with the first order because they are diffracted at different angles, and can be separated geometrically. However, the spectral purity of the first order can be degraded for another reason; if the acoustic wave travelling through the Bragg-cell is not totally absorbed at the edge of the crystal, there remains a reflected component travelling in the opposite direction along the crystal. This acoustic component will frequency shift part of the light, in the opposite sense. Effectively, it generates two other optical beams that contribute to the set of interference phenomena on the photodetector. This effect can yield up to 10 % of instability.

(iii) *Effect due to the laser modes*

The He–Ne laser of the probe lases on several modes at different frequencies. As a result, yet more interference effects are obtained on the photodetector, leading to new electrical frequency components. Spurious components, giving rise to instabilities, are obtained when nonlinearities are encountered in the subsequent electronics. However, less than 0.1 % of instability is expected from this effect.

2.2. *A modified probe design*

Figure 3 shows a modified design, where the laser beam passes only once through the Bragg cell. Here, a polarizing beam splitter, enables one to separate the incident and reflected beam from the object, which are colinear because of the focusing lens. The $\frac{1}{4}\lambda$ plate rotates the polarization of the linear polarized beam by 90°, so that the beam is directed to the detector after reflection from the object. The two beams coming from the beam splitter to the detector are linearly polarized with an angle of 90° between them, so that they will not interfere. An additional polarizer, orientated at 45° relative to the two polarization vectors, extracts from the two beams two polarization components that are parallel. The requirement in angular

PHILOSOPHICAL TRANSACTIONS OF THE ROYAL SOCIETY A MATHEMATICAL, PHYSICAL & ENGINEERING SCIENCES

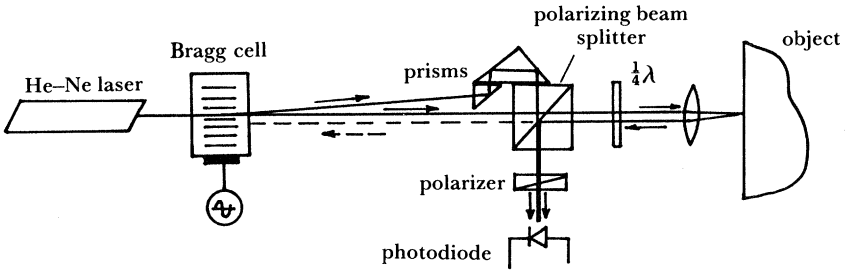

FIGURE 3. New configuration of the laser probe.

alignment for the two beams incident on the photodetector is very strict (De la Rue *et al.* 1972); in a typical experimental arrangement, an angle smaller than 10^{-4} between them is required. This configuration, where the reference passes through the polarizing prism, facilitates the alignment of the two beams.

Compared with the present probe, this new design brings a number of advantages.

(i) It is possible greatly to reduce the instability due to the first effect. By slightly off-centring the lens (figure 3), incident and reflected beams follow a different path. This enables one to stop any spurious beam to return to the laser.

(ii) Calculations showed that the instabilities due to the second effect are avoided.

(iii) The arrangement is more compact; the laser can be positioned close to the Bragg cell.

(iv) The carrier frequency generated in the photo-detector is the Bragg-cell frequency f_B (and not $2f_B$); this simplifies the electronic detection.

Preliminary results have shown that the level of instabilities are reduced to about 1%. Further work will be concerned with the use of a beamsplitter with improved separation ratio in order to reduce the residual optical intensity that could return toward the laser. The optical alignment has also become easier since the two beams do not need to pass twice through the Bragg cell, as in the previous design. In addition, the available optical power at the photodetector is larger, compared with that of the previous configuration, giving a 5 dB increase of the photodetector current.

3. EXPERIMENTAL RESULTS

The photodisplacement technique allows the non-destructive examination of structures and defects in the near-surface region of samples such as crystals, semiconductors, or integrated circuits. The examination can be effected on a microscopic scale. The samples are scanned in a raster fashion under the two laser spots which remain stationary. In all the following experiments, the heating semiconductor laser produced a peak power of 2 mW at 820 nm, focused into a 8 μm diameter spot, and modulated at 10 kHz. The resulting surface displacement is between 0.1 and 1 Å.

3.1. *Thin film thickness measurement*

In a solid, the interaction of thermal waves is limited to a region near the surface. One can exploit this property for thin-film thickness measurements. Several detection methods have been implemented for this purpose (Rosencwaig *et al.* 1983; Williams 1984) with sensitivities that allowed measurements in a range from 20 Å to 2 μm. Figure 4 shows the phase of the photodisplacement signal recorded over a film of aluminium of varying thickness, deposited

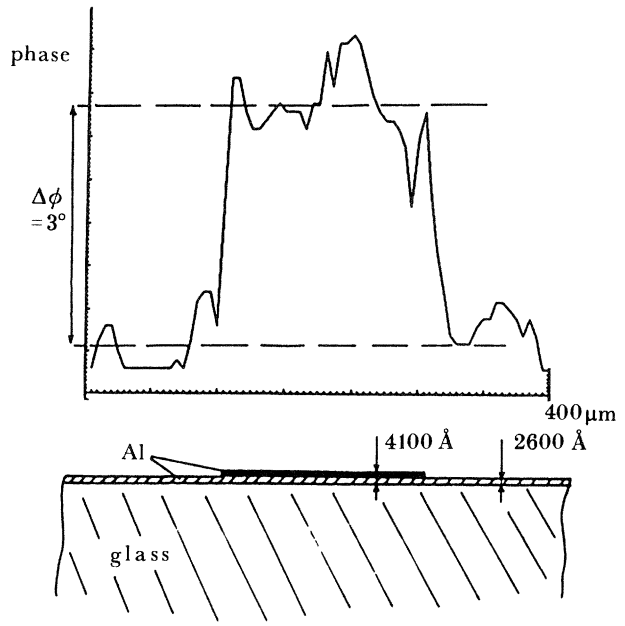

FIGURE 4. Measurement of aluminium film thickness.

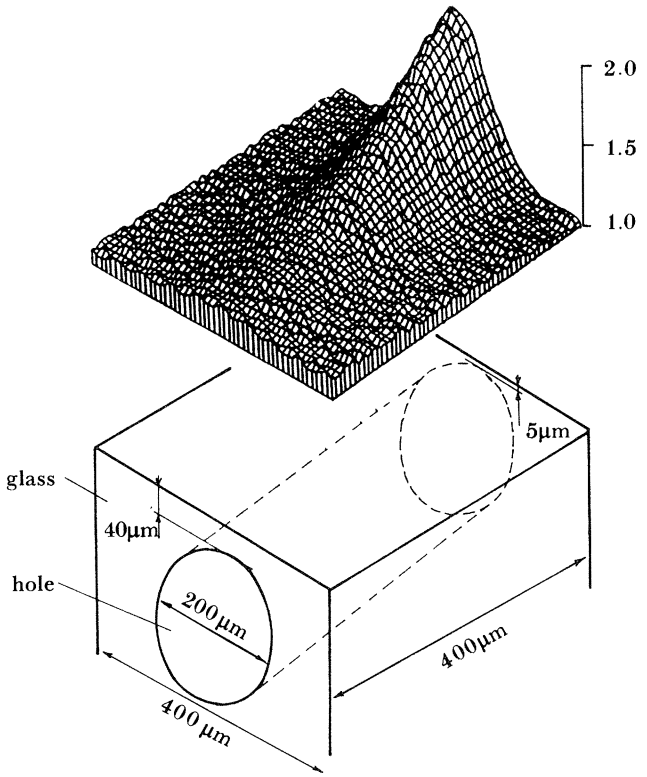

FIGURE 5. Detection of a subsurface hole in glass.

PHILOSOPHICAL TRANSACTIONS OF THE ROYAL SOCIETY A MATHEMATICAL, PHYSICAL & ENGINEERING SCIENCES

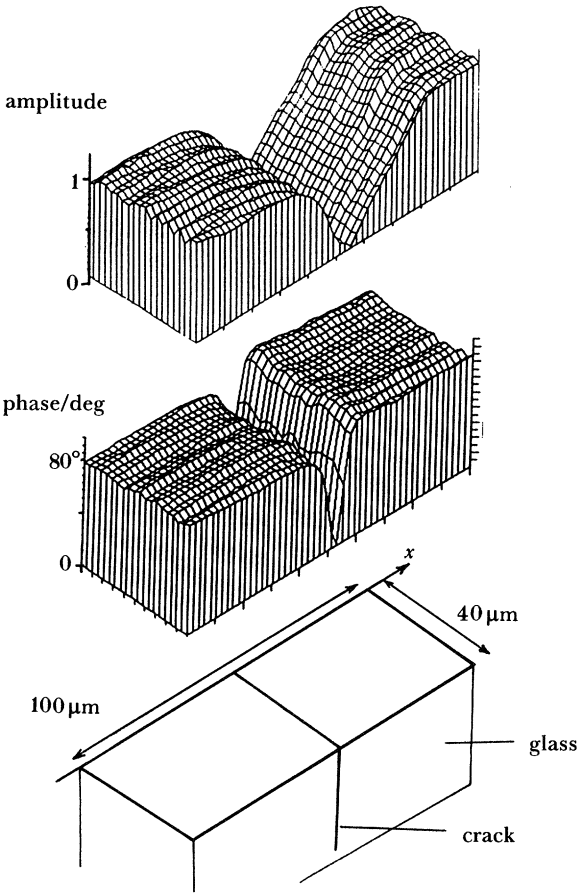

FIGURE 6. Imaging of a surface breaking crack in glass.

on a glass substrate. The phase variation is 3° for a thickness variation of 1500 Å. One can deduce that a probe stability of 0.1° would allow the detection of a thickness variation of 50 Å.

3.2. *Examination of a subsurface hole*

A circular hole, described in figure 5 was drilled in a block of glass; the top surface of the block was polished and covered with a thin layer (0.1 µm) of aluminium. The hole was detected at a depth varying between 5 and 40 µm; the increase of the photodisplacement amplitude was 100 to 9% respectively. However, from a simple one-dimensional theory, one should not expect such a large increase as 9% at a depth of 40 µm. The thermal diffusion length in glass is 4.4 µm at the modulating frequency of 10 kHz; at a depth of 40 µm, the thermal wave has decreased by a value larger than 10^4 and the contribution from the reflected wave to the surface displacement cannot explain the measured 9% increase. A possible explanation could be the presence of microcracks surrounding the hole, a surmise which, we shall see, is supported by further experiments presented in §3.4.

3.3. *Detection of surface-breaking cracks*

Surface-breaking cracks have been detected in a block of glass (figure 6) when the heating and probing beams are separated by 20 µm (Martin & Ash 1984*a*). Such a separation

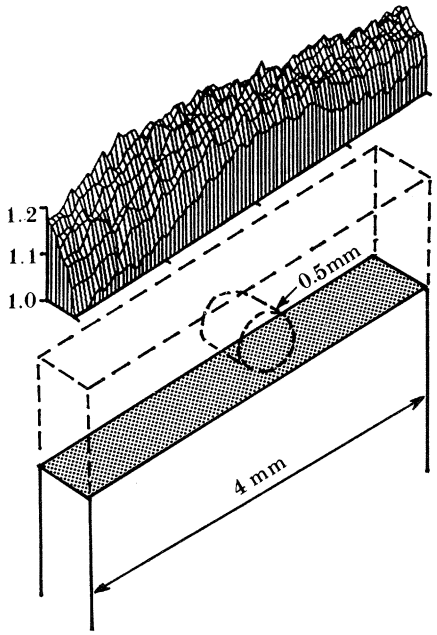

FIGURE 7. Detection of microcracks induced by an ultrasonic drill in glass.

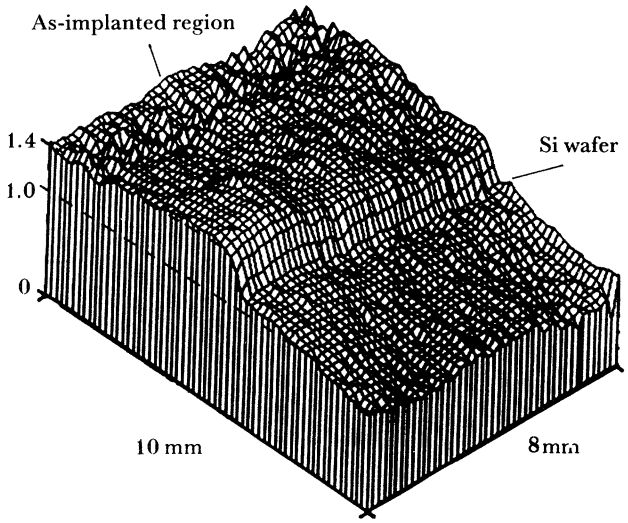

FIGURE 8. Imaging of an arsenic-implanted silicon wafer.

between the two laser beams increases the sensitivity of the technique by a factor larger than five; the crack hinders the lateral propagation of the thermal wave from the heating to the probing beam, and is thereby readily detected.

3.4. *Detection of micro-cracks in glass*

Some calculations have demonstrated the importance of the effect of elastic deformations to the photo-displacement signal over surface breaking cracks (Martin & Ash 1984*b*) and over a subsurface hole (Olmstead *et al.* 1983). From these examples, the technique appears to be particularly sensitive for the detection of physical defects, such as cracks or flaws.

PHILOSOPHICAL TRANSACTIONS OF THE ROYAL SOCIETY A MATHEMATICAL, PHYSICAL & ENGINEERING SCIENCES

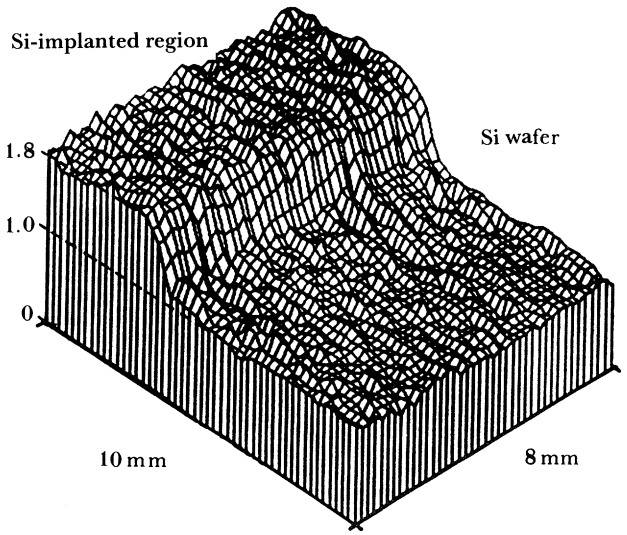

FIGURE 9. Imaging of a silicon-implanted silicon wafer.

The subsurface hole of § 3.2 was drilled with an ultrasonic vibrating tool; this drilling process can be responsible for the formation of microcracks in the region near the hole. Such microcracks would modify the elastic deformation of the heated region of the glass. In order to confirm this possible explanation, we performed further investigation on this sample: we polished the top surface (figure 7) so as to eliminate the hole from the glass block. No microcracks or inhomogeneities were observed under the optical microscope, that could any longer reveal the presence of the previous hole. We then covered the top surface with a thin layer of aluminium (0.1 μm) and scanned it under the two laser beams. Figure 7 shows the result: an increase of 10 % of the photodisplacement amplitude was obtained over the area near the previous hole, where microcracks were expected. This result confirms the remarkable sensitivity of the photodisplacement technique to physical defects such as microcracks, a sensitivity that can be attributed to an effect of elastic deformations modified by the presence of microcracks.

3.5. *Observations of ion implanted regions in silicon*

Microcracks and subsurface damage are obtained as a result of ion implanation in semiconductors. Therefore, we have used the photodisplacement technique for the observation of ion implanted regions in silicon. The first test sample was a silicon wafer, half of its surface being implanted with arsenic at a dosage of 10^5 cm^{-2} and with an energy of 180 kV. Figure 8 shows the amplitude of the photodisplacement signal recorded over the wafer. The amplitude of the signal over the implanted region is 40 % larger than over the nonimplanted region. The origin of such an increase has not yet been determined. However, to separate the effect of the arsenic ions themselves, we examined another silicon wafer, implanted with silicon, and under the same conditions as the previous sample. This time, an increase of 80 % was obtained (figure 9). This result reinforces our belief that the photodisplacement technique is very sensitive to damage associated with ion implantation.

4. Further instrumental development: photodisplacement microscopy with the use of a single laser

We have investigated photodisplacement microscopy with the use of two lasers. Several other techniques for photothermal displacement spectroscopy, such as the beam deflection technique of the attenuated total reflection detection, also need two lasers, called the pump laser and the probe laser (Olmstead *et al.* 1983). We shall introduce a novel configuration using a single laser for photodisplacement. The same optical beam serves both to heat the object and to measure the resulting surface displacement. As a result there is a notable simplification in the required optical arrangement. Moreover, the probing beam will always be positioned at the centre of the heated spot; this will obviate the need for the critical alignment of the two laser beams.

4.1. *Experimental implementation*

Keeping the present configuration of the laser probe (figure 10), the AC heating of the object can be obtained by modulating the probe beam intensity. An external modulator can be added at the output of the He–Ne laser. However, the configuration of the probe provides a simpler way of obtaining the required amplitude modulation on the object. The existing Bragg cell, in addition to its functions of beam splitting and optical frequency conversion is also capable of modulating the amplitude of the light incident on the object. By amplitude modulating the input current of the Bragg cell, one amplitude modulates the light intensity coming out on the zero and on the first order.

The major difficulty is to find a possible way to extract the wanted signal from the complex photodetector current. By judicious modulation of the laser beam, a square-wave modulation, we discovered that it is possible to identify a harmonic in the spectrum of the current which is proportional to the surface displacement. Let M_0 and M_1 be the modulation factors of the zero- and first-order beams that pass through the Bragg cell, respectively. For a square-wave modulation, M_0 and M_1 can be written as:

$$M_0 = a_0 - a_0' \left(\frac{\cos \omega_m t - \frac{1}{3} \cos 3\omega_m t + \frac{1}{5} \cos 5\omega_m t - \dots}{\arctan 1} \right),$$

$$M_1 = a_1 + a_1' \left(\frac{\cos \omega_m t - \frac{1}{3} \cos 3\omega_m t + \frac{1}{5} \cos 5\omega_m t - \dots}{\arctan 1} \right),$$

where a_0, a_1, and a_0, a_1 are the average and peak optical intensities of the square-modulated beams; the expansion of the cosine terms represents the square-wave modulation.

With the previous notations, the two interfering beams on the photodetector become $R \cdot (M_0 \cdot M_1)^{\frac{1}{2}}$ and $S \cdot (M_0 \cdot M_1)^{\frac{1}{2}}$. Hence, the photodetector current, I, becomes:

$$\begin{aligned} 1 &= (R+S)\,(R+S)^* \cdot M_0 \cdot M_1 \\ &= \alpha \cos(2\omega_b t + \phi) + \tfrac{1}{2} kdb \left[\sin(2\omega_b t + \phi_m + \phi) + \sin(2\omega_b t - \phi_m + \phi)\right] \\ &\quad + \tfrac{1}{2} b \left[\cos\{(2\omega_b + \omega_m) t + \phi\} + \cos\{(2\omega_b - \omega_m) t + \phi\}\right] \\ &\quad + kd\alpha \left[\sin\{(2\omega_b + \omega_m) t + \phi_m + \phi\} + \sin\{(2\omega_b - 2\omega_m) t - \phi_m + \phi\}\right] \\ &\quad + \tfrac{1}{2} kdb \left[\sin\{(2\omega_b + 2\omega_m) t + \phi_m + \phi\} + \sin\{(2\omega_b - 2\omega_m)\, t - \phi_m + \phi\}\right. \\ &\quad \left. - \tfrac{1}{3} \sin\{(2\omega_b + 2\omega_m)\, t - \phi_m + \phi\} - \tfrac{1}{3} \sin\{(2\omega_b - 2\omega_m) t + \phi_m + \phi\}\right] \\ &\quad + \tfrac{1}{6} a \left[\cos((2\omega_b + 3\omega_m) t + \phi) + \cos\{(2\omega - 3\omega_m) t + \phi\}\right] \end{aligned}$$

PHILOSOPHICAL TRANSACTIONS OF THE ROYAL SOCIETY A MATHEMATICAL, PHYSICAL & ENGINEERING SCIENCES

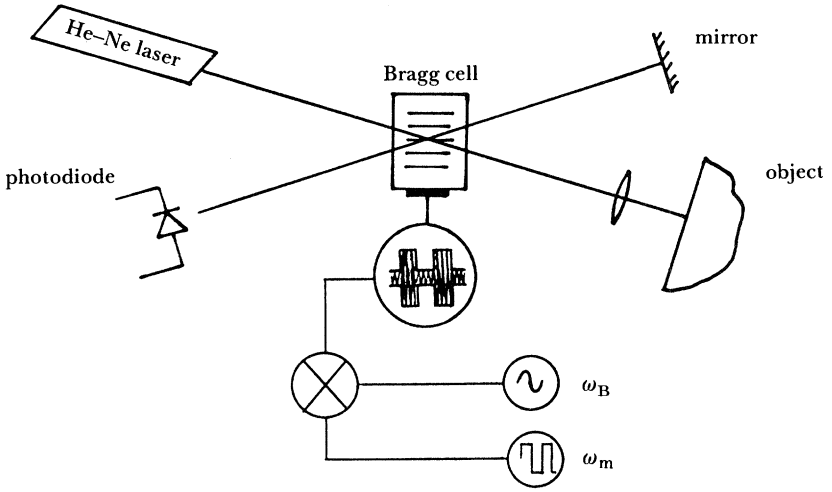

FIGURE 10. Optical configuration for photodisplacement microscopy with the use of a single laser.

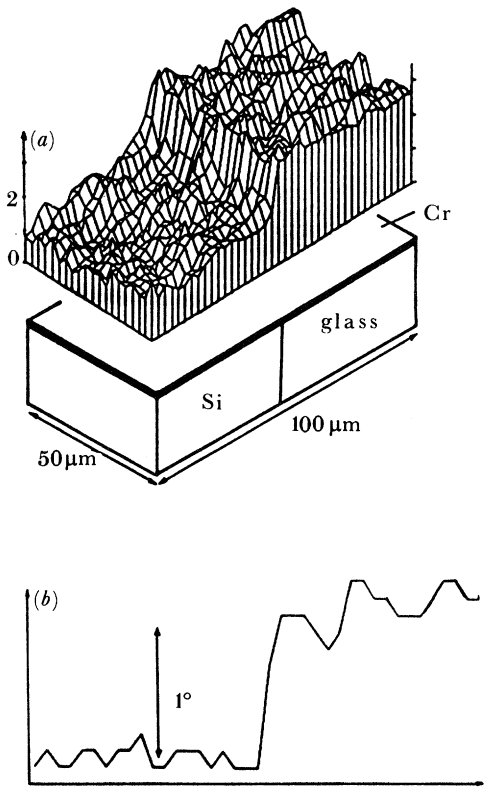

FIGURE 11. Imaging of a silicon–glass butt joint covered with chromium by photodisplacement microscopy with the use of a single laser, (*a*) amplitude (*b*) phase.

where

$$a = a_0\, a_1\, \tfrac{1}{2} a_0'\, a_1', \quad b = \left(\frac{a_0\, a_1' - a_1\, a_0'}{\arctan 1}\right), \quad \phi = \phi_R - \phi_S.$$

We notice that the amplitude of the second-order side bands of I, at frequencies $2\,\omega_b \pm 2\,\omega_m$, depends only on the surface displacement d, via optical wavenumber k. By carefully filtering

the complex current, we extracted this component and mixed it with the carrier frequency of the current. From the resulting signal, we obtained the amplitude and phase of the surface displacement.

4.2. *Experimental result*

We carried out an experiment to demonstrate the sensitivity of the technique to thermal contrasts in objects. The sample consisted of a butt joint of glass silicon, the top common surface being polished and covered with a chromium film of 0.2 μm thickness to eliminate any optical contrast (figure 11). The three-dimensional diagram shows the amplitude of the photodisplacement signal over the butt joint. We used a 6 mW He–Ne laser and the modulation frequency was 7 kHz. A signal-to-noise ratio of around two is obtained. By averaging the phase signal 20 times over the sample, the noise is reduced so that the two regions become clearly visible on the line scan of figure 11.

Here again, instabilities have appeared, of the same nature as those discussed for the probe instability (§1). These are the reason of the random variations seen over each area of the butt joint. We believe that the new laser-probe configuration, described in §2.2, will provide the basis for the new photodisplacement instrument using a single laser. The improved stability should allow the detection of signal changes much smaller than 1%.

5. Conclusion

The use of an interferometric laser probe is the basis of the high sensitivity demonstrated for the photodisplacement technique. A heating power of the order of milliwatts yields a probe signal: noise ratio larger than 10^3. The defect detection threshold is, however, related to the stability of the probe. The new optical configuration of the instrument allows the observation of changes in the photodisplacement signal much smaller than 1%.

We have observed that the photodisplacement signal itself is strongly affected by the presence of physical defects in materials, such as voids or microcracks. This particular sensitivity is attributed to the response to *elastic deformations*, which is a unique feature of the photodisplacement technique. A strong signal has been recorded over ion-implanted silicon regions, and it is anticipated that the technique will find a range of applications on the examination of semiconductor materials. The spatial resolution approaches optical resolution; it is enhanced by the fact that both generation and detection of the thermal wave operate via a focused laser beam.

New instrumental developments have led to a novel and simpler optical configuration using a single laser.

The authors thank Professor E. Dieulesaint and Dr D. Royer for fruitful discussion on the design of laser probes. One of us (Y.M.) gratefully acknowledges the receipt of a grant from the Royal Society Paul Instrument Fund.

References

Bowers, J. E., Jungerman, R. L., Khuri-Yakub, B. T. & Kino, G. S. 1983 An all fiber-optic sensor for surface acoustic wave measurements. *J. Lightwave Tech.* **LT-1** (2), 429–436.

De la Rue, R. M., Humphreys, R. F., Mason, I. M. & Ash, E. A. 1972 Acoustic-surface-wave amplitude and phase measurements using laser probes. *Proc. IEE* **119** (2), 117–126.

Jungerman, R. L., Bowers, J. E., Green, J. B. & Kino, G. S. 1982 Fiber optic laser probe for acoustic wave measurements. *Appl. phys. Lett.* **40**, 313–315.

PHILOSOPHICAL TRANSACTIONS OF THE ROYAL SOCIETY A MATHEMATICAL, PHYSICAL & ENGINEERING SCIENCES

Kwaaitaal, T., Luymes, B. J. & Van der Pijll, G. A. 1980 Noise limitations of Michelson laser interferometers. *J. Phys.* D **13**, 1005–1015.

Martin, Y. & Ash, E. A. 1984*a* Displacement detection techniques for thermal wave non-destructive testing. In *Proceedings of the 2e Colloque sur la diffusion des ondes ultrasonores, Paris, December 1984*. Traitement du Signal. (In the press.)

Martin, Y. & Ash, E. A. 1984*b* Imaging of micro-cracks by photodisplacement microscopy. In *Proc. IEEE Ultrasonics Symp., Dallas, November 1984*.

Olmstead, M. A., Amer, N. M., Kohn, S., Fournier, D. & Boccara, A. C. 1983 Photothermal displacement spectroscopy: an optical probe for solids and surfaces. *Appl. Phys.* A **32**, 141–154.

Olsson, A., Tang, C. L. & Green, E. L. 1980 Active stabilisation of a Michelson interferometer by an electro-optically tuned laser. *Appl. Opt.* **19** (12), 1987–1899.

Rosencwaig, A., Opsal, J. & Willenborg, D. L. 1983 Thin film thickness measurements with thermal waves. *J. Phys.*, Paris C**6**, 483–489.

Whitman, R. L. & Korpel, A. 1969 Probing of acoustic surface perturbations by coherent light. *Appl. Opt.* **8** (8), 1567–1576.

Williams, C. C. 1984 Thin film characterisation with optical resolution using 1GHz thermal waves. In *Proc. IEEE Ultrasonic Symp.* (In the press.)

Discussion

G. Busse (*I.K.P., Universität Stüttgart, F.R.G.*) I understand that surface topography does not affect signal detection very much. On the other hand, reflection is needed. Does that mean that only metallic samples can be inspected?

Y. Martin. One can inspect metallic or non metallic samples such as glass or quartz, etc. The reflected He–Ne laser light from a glass sample (4% of the incident intensity) is enough to allow the laser probe to function in reasonable conditions.

R. S. Gilmore (*General Electric Company, Corporate Research and Development, New York 12301, U.S.A.*). How long does it take for an image to be produced?

Y. Martin. Most of the pictures can be taken in less than one minute.

PHILOSOPHICAL TRANSACTIONS OF THE ROYAL SOCIETY A MATHEMATICAL, PHYSICAL & ENGINEERING SCIENCES